Biosensors and Bioelectronics 142 (2019) 111539

Contents lists available at ScienceDirect

Biosensors and Bioelectronics

journal homepage: www.elsevier.com/locate/bios

Electrochemical immunosensor based on gold-labeled monoclonal anti-LipL32 for leptospirosis diagnosis

Sakda Jampasa[a], Prayoon Lae-ngee[b], Kanitha Patarakul[b], Nattaya Ngamrojanavanich[c], Orawon Chailapakul[d,e], Nadnudda Rodthongkum[a,*]

[a] Metallurgy and Materials Science Research Institute, Chulalongkorn University, Pathumwan, Bangkok, 10330, Thailand
[b] Department of Microbiology, Faculty of Medicine, Chulalongkorn University, Pathumwan, Bangkok, 10330, Thailand
[c] The Institute of Biotechnology and Genetic Engineering, Chulalongkorn University, Patumwan, Bangkok, 10330, Thailand
[d] Electrochemistry and Optical Spectroscopy Research Unit, Department of Chemistry, Chulalongkorn University, Pathumwan, Bangkok, 10330, Thailand
[e] National Center of Excellence for Petroleum, Petrochemicals, and Advanced Materials, Chulalongkorn University, Pathumwan, Bangkok, 10330, Thailand

ARTICLE INFO

Keywords:
Electrochemical immunosensor
LipL32
Screen-printed graphene electrode
Graphene oxide
Gold-labeled antibody

ABSTRACT

Leptospirosis is a critical human health problem in the tropical area, thus, a precise technique that can be used for point-of-care analysis is greatly required. This is the first report on electrochemical immunosensor based on gold-labeled monoclonal anti-LipL32 for rapid, simple and sensitive determination of LipL32. The sensor consisted of two LipL32-specific antibodies: an unlabeled capture primary antibody (Anti-1°Ab) and an electrochemically detectable gold-conjugated secondary antibody (Au-2°Ab). The Anti-1°Ab was immobilized onto the modified screen-printed graphene electrode (SPGE) to form the anti-LipL32 surface. The electrochemical signal response was determined by differential pulse voltammetry (DPV). In the presence of LipL32, the sensor displayed a significant increase in current response in a concentration-dependent manner, but no observable signal was detected in the absence of LipL32. The linearity between LipL32 concentration and the measured current was found in a range of 1–100 ng/mL, and the limit of detection (LOD) ($3SD_{blank}$/Slope) and limit of quantitation (LOQ) ($10SD_{blank}$/Slope) were found to be 0.28 and 0.93 ng/mL, respectively. This sensor was successfully applied to detect pathogenic *Leptospira* whole cell lysates samples with the satisfactory results. The promissing results suggested that this immunosensor might be an alternative tool for diagnosis of leptospirosis.

1. Introduction

Leptospirosis, a global zoonotic disease caused by pathogenic *Leptospira*, is a crucial human health problem in the tropical areas (Bharti et al., 2003). In the past decades, human cases of leptospirosis have dramatically increased, and among these cases are from patients who live in the regions with limited public healthcare resources (Goarant, 2016). The pathogenic *Leptospira* infection is typically transmitted to humans through exposure with water or soil polluted with the urine of infected animals. To date, the controls of a zoonotic disease have received much concern worldwide.

Leptospirosis can cause mild to severe clinical manifestations, such as fever, headache, myalgia, conjunctival suffusion, hepatomegaly, pulmonary hemorrhage, jaundice, and renal failure (Daher et al., 2014). Nevertheless, at the early stage of illness, the clinical features of leptospirosis are non-specific and difficult to distinguish from other infectious diseases. Therefore, the laboratory tests are required to confirm the diagnosis and indicate appropriate treatment, which is crucial for morbidity and mortality rate (Budihal and Perwez, 2014). Hence, the efficiency and accuracy of the pathogen identification is essential. Various specimens such as blood, urine and/or relevant fluids are often employed as the target samples for *Leptospira* culture (Musso and La Scola, 2013). However, leptospiral culture requires special media and may take up to 4 weeks to report due to slow growth rate resulting in low sensitivity and delayed diagnosis.

To date, numerous techniques have been established for leptospirosis diagnosis, such as IgM Enzyme-Linked Immunoassay (IgM ELISA), Microscopic Agglutination Test (MAT), Dark Field Microscopy (DFM), Polymerase Chain Reaction (PCR) (Budihal and Perwez, 2014; Musso and La Scola, 2013). One of the most common targets of detection is LipL32, a major outer membrane protein (OMP) of pathogenic *Leptospira* grown in vitro and in vivo (Haake et al., 2000; Hoke et al., 2008; Sumarningsih et al., 2016). Nonetheless, these techniques still possess some limitations. The drawback of IgM assay is lack of

* Corresponding author.
E-mail addresses: corawon@chula.ac.th (O. Chailapakul), nadnudda.r@chula.ac.th (N. Rodthongkum).

https://doi.org/10.1016/j.bios.2019.111539
Received 16 May 2019; Received in revised form 9 July 2019; Accepted 25 July 2019
Available online 26 July 2019
0956-5663/

sensitivity and false positive detection because IgM antibodies can persist in blood for several months. Although MAT is currently a standard method for diagnosis of leptospirosis, its performance is limited to reference laboratories as there is a need to preserve a panel of viable leptospiral strains for preparing antigens. This method is labor intensive and requires uncommonly available instrument. The disadvantages of DFM is low sensitivity and specificity. PCR requires expensive reagents and instruments (Budihal and Perwez, 2014). Hence, these techniques are unsuitable for countries with inadequate resources. Therefore, the novel detection methods offering simplicity, high sensitivity, and rapidity are still greatly required for primary medical diagnosis and controlling of the disease.

Electrochemical detection is an attractive alternative technique for practical application in primary medical diagnosis due to its several advantages for point-of-care testing (Hammond et al., 2016; Huang et al., 2017; Wang, 2006; Zhang and Liu, 2016). The electrochemical immunosensor can be categorized into two detection modes: "signal-on" and "signal-off (Kuang et al., 2010; Wu and Lai, 2013). The "signal-on" mode provides a much-improved signal compared to the "signal-off" mode, which inherently suffers from limited signaling capacity to a maximum of 100% signal suppression. The small signal change could be difficult to detect due to the presence of large background signal from the initial signal, leading to false-positive results (Anne et al., 2003; Mao et al., 2003; Wu and Lai, 2015). To eradicate these limitations, it is more desirable to develop a "signal-on" detection method. Up to now, electrochemical measurement has been applied in many applications, especially in biologica analyses (De Souza and Machado, 2005; Emran et al. 2018a, 2019; Emran et al., 2018e; Emran et al., 2018f; Goyal et al., 2006; Hammond et al., 2016; Jampasa et al., 2014). However, so far there is no available electrochemical sensor to detect LipL32 protein of pathogenic *Leptospira*.

Hence, our aim is to introduce a novel electrochemical sensor for a simple and highly selective determination of LipL32. A sandwich-type format was implemented for the formation of Anti-1˚Ab, LipL32 and the Au-2˚Ab. The presence and absence of LipL32 was monitored by observing the signal response of gold conjugated on the secondary antibody. To successfully fabricate the electrochemical immunosensor, a disposable SPGE was used. The analytical performances including the sensitivity, specificity, and reproducibility of the developed immunosensors were evaluated. Finally, this LipL32 immunosensor was applied to detect pathogenic *Leptospira* whole cell lysates.

2. Experimental

2.1. Chemicals, apparatuses and measurements

Details of chemicals, apparatuses and measurements are presented in Supplementary Information (SI).

2.2. Production and purification of monoclonal antibodies

Details of antibodies production, purification and source can be found in SI (Figs. S1 and S2).

2.3. Fabrication of the SPGE

The disposable SPGE was fabricated using an in-house screen-printing technique as previously described (Jampasa et al., 2016). The design and fabrication process of SPGE are described in SI (section 1.6, Fig. S3).

2.4. Preparation of the LipL32 immunosensor and electrochemical measurement

In this present work, a selective sandwich-type assay format was employed (Izumi et al., 1991; Jampasa et al., 2018a). The sensor is comprised of two LipL32-specific monoclonal antibodies, one with a label and another one is unlabeled. The importance and advantages of using monoclonal antibodies in the diagnostic test are their high specificity, minimal background noise and cross-reactivity, long-term continuous production as the source of reagents, and high consistency of the result (minimal lot-to-lot variation) (Bayat et al., 2015). For the immobilization step, an unlabeled Anti-1˚Ab was covalently attached onto the electrode surface using the standard EDC/sulfo-NHS chemistry since it provides the direct conjugation of GO carrying a carboxylic group (–COOH) to the primary amine groups ($–NH_2$) on the antibodies (Raghav and Srivastava, 2016). Prior to modification, the electrode surface was cleaned extensively with Milli-Q water, followed by a drop-casting of a 0.5 mg/mL GO (2.5 µL) dispersed in dimethyl formamide (DMF) media. This modified electrode was then left to dry at RT and denoted as GO-SPGE. After drying, GO-SPGE was further anodized in 0.5 M NaOH with a constant potential of +1.3 V for 40 s to enlarge the number of carboxylic group on GO sheets (Wei et al., 2007). The anodized GO-SPGE surface was then treated with the solution containing 50 mM EDC and 30 mM sulfo-NHS (4 µL), prepared in MES pH 4.7, and incubated at RT for 1 h. The activated surface was rinsed twice with PBS to remove the unreacted EDC/sulfo-NHS. After this step, the carboxyl group was converted to the amine-reactive sulfo-NHS ester which is ready for the next immobilization step. The capture anti-LipL32 solution (100 µg/mL, 2.5 µL) was dropped onto the sulfo–NHS–activated surface and left overnight in a sealed small box to prevent the evaporation of the solution, at 4 °C. This electrode was left overnight to allow immobilization of antibody complete. The Anti-1˚Ab-GO-SPGE electrodes were then thoroughly washed with PBS twice to remove the excess and non-specifically adsorbed antibody on the electrode surface. After that the nonspecific binding sites on the electrode surface were blocked via casting of 5% (w/v) skim milk (SKI) (3 µL) solution at the same temperature for overnight. These electrodes were denoted as AB1-SKI-GO-SPGE. For LipL32 binding step, the solution of purified recombinant LipL32, pathogenic or non-pathogenic *Leptospira* whole cell lysates (2.5 µL) at the designated concentration was dropped onto the WE and left for 50 min, followed by the extensive washing with 0.5% Tween in PBS. The added Tween can enhance the efficiency of this washing step, resulting in the decreased background signal and the non-specific adsorption on the electrode surface. After capturing of LipL32, the solution of Au-2˚Ab (10 µg/mL, 2.5 µL) was subsequently dropped onto the electrode surface and left for 50 min. The modified electrode was then rinsed with PBS to remove the excess signaling antibody. 0.5 M HCl (40 µL) was finally dropped onto the electrode surface again prior to the electrochemical measurement. Preparations of the LipL32 immunosensor is summarized in Scheme 1.

2.5. Sample preparation

Details of sample preparation is presented in SI, section 1.7.

3. Results and discussion

3.1. Characterization of the modified SPGE

To verify the success of sensor fabrication, the appropriate characterizations such as SEM, EIS and FTIR techniques were used. The surface morphologies of the modified and unmodified electrodes were investigated by SEM. As shown in Fig. 1B, after drop casting of GO, the surface became a tissue-like structure and free from cracks with crumbled film covered the electrode surface, while the unmodified electrode showed few flakes of graphene sheets (Fig. 1A). In addition, after the immobilization of a monoclonal anti-LipL32 (Fig. 1C), the image depicts the change in surface morphology of electrode with a smoother and less wrinkle compared to the GO-SPGE, indicating the successful immobilization of biomolecules on the electrode surface (Wang et al., 2014). Moreover, to confirm an enlargement of carboxylic

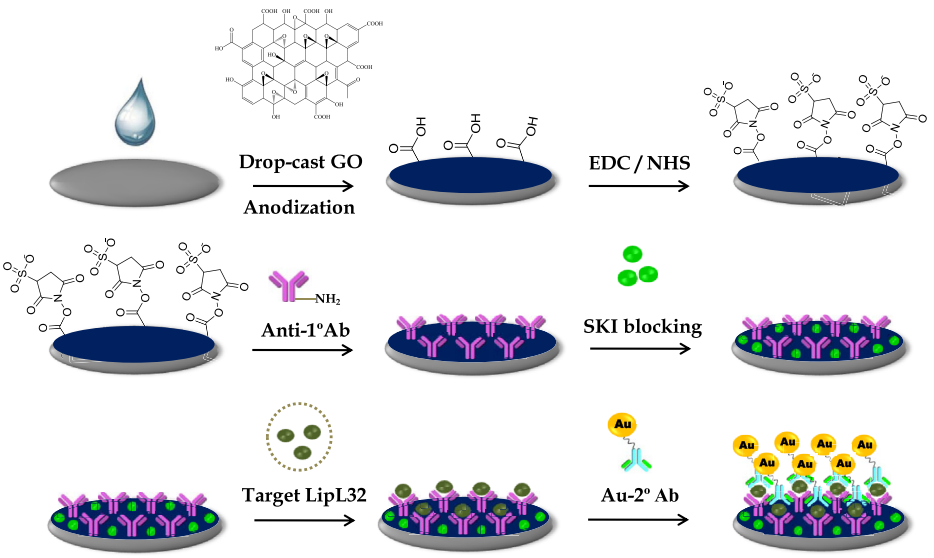

Scheme. 1. Schematic illustration of the immunosensor fabrication for detecting LipL32.

group on the electrode surface, FTIR was carried out. The FTIR spectrum of the GO-SPGE presented all of the characteristic bands for GO including: C = O stretching at 1716 cm^{-1}, C–O stretching at 1045 cm^{-1}, and finally the OH stretching at 3205 cm^{-1} (Fig. 1D, dash line) (Basirun et al., 2013). The FTIR of the anodized GO-SPGE preserved all the characteristic bands of GO, except that the peak due to OH and C = O stretching remarkably increased (Fig. 1D, blue line). This result indicates an enlargement of C = O functional group on the GO sheets. Moreover, the electrochemical measurement of dissolved dopamine (DA) solution in mild acidic condition was also conducted to further confirm the presence of carboxylate groups ($-COO^-$) on the anodized GO-SPGE electrode (Wei et al., 2007). The results exhibited the DA current considerably increased at the anodized GO-SPGE in comparison to the non-anodized electrode (Figs. S4 and SI). This signal amplification can be described by the attraction of the positive charge of DA molecules being attracted to the electrode surface with the negative charged carboxylate groups, making it more accessible for the DA molecule (Wei et al., 2007).

In addition, the Raman shift was also carried out to confirm the modified SPGE surface with GO. As shown the Fig. 1E, the Raman spectra of SPGE (brown line) displayed very small both D and G bands at ~1320 cm^{-1} and ~1600 cm^{-1}, corresponding to the symmetry A_{1g} mode and the E_{2g} mode of sp^2 carbon atoms, respectively. Similarly, the Raman spectra of GO-SPGE preserved all the D and G bands (blue line), except that the peak due to D and G intensity obviously enlarged, indicating the deposition of GO on SPGE (Jabbar et al., 2017; Stankovich et al., 2007; Zhang et al., 2010).

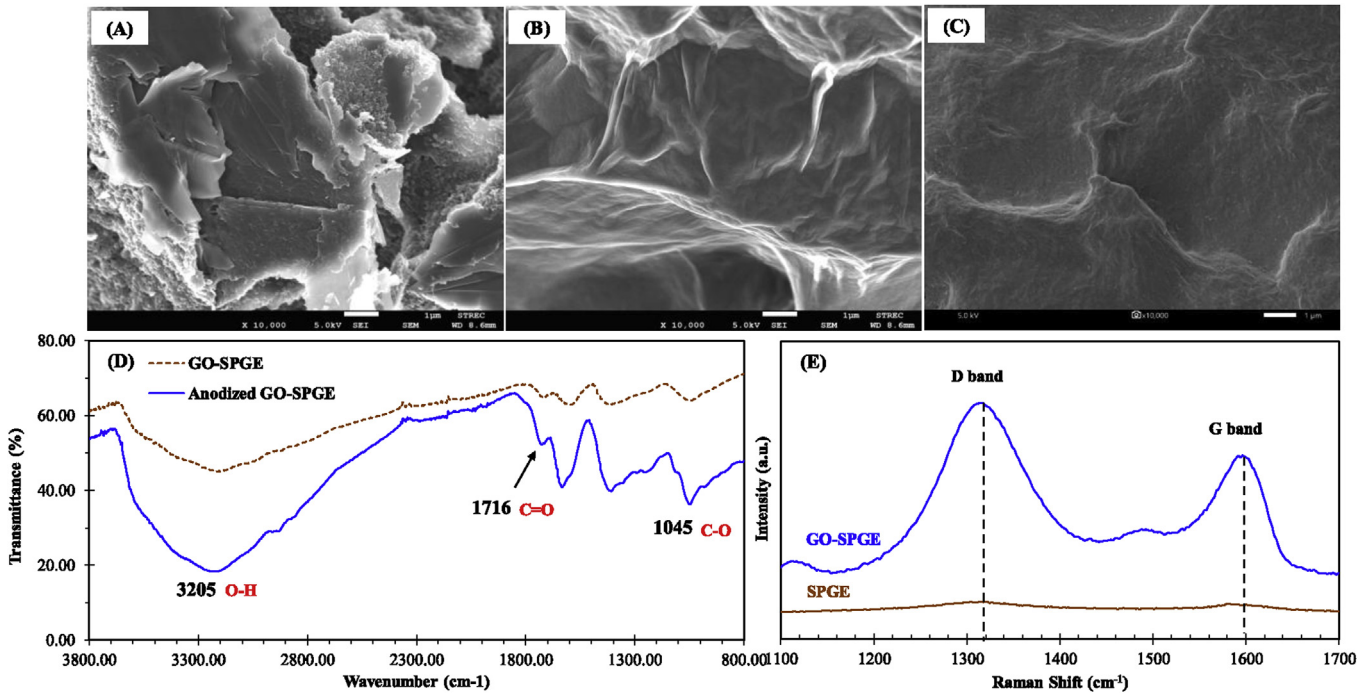

Fig. 1. SEM images of an unmodified (A), GO-modified SPGE (B) and AB1-GO-SPGE (C). FTIR spectra of the GO-SPGE and anodized GO-SPGE (D). Reman spectra of the SPGE and GO-SPGE (E).

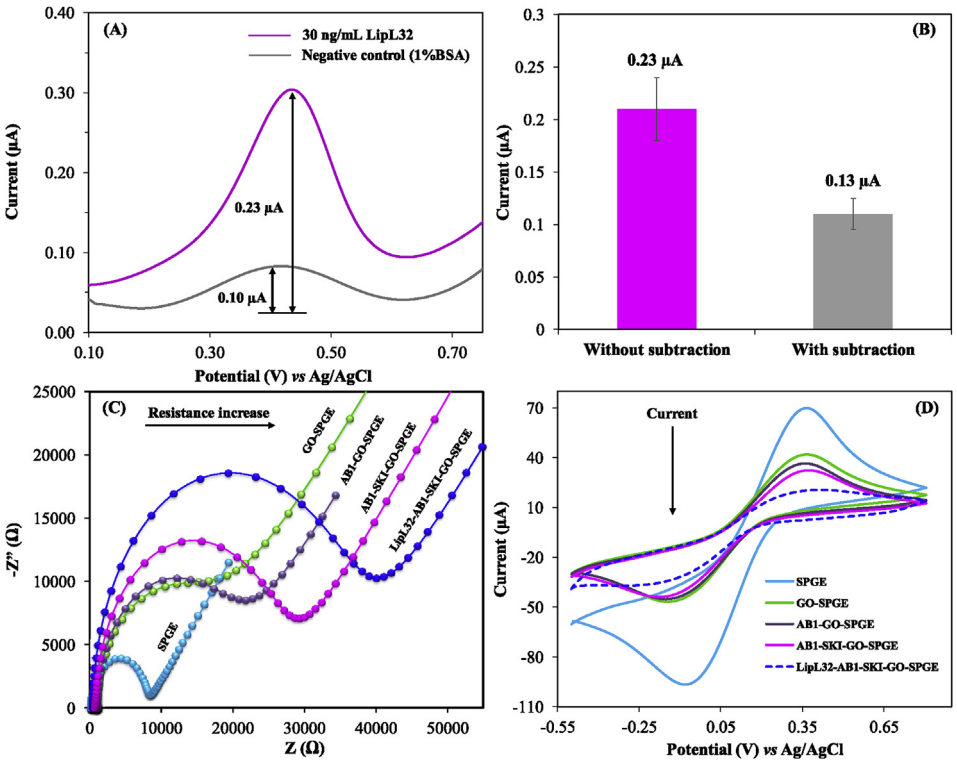

Fig. 2. DPV responses of the AB1-SKI-GO-SPGE after addition of the target protein (30 ng/mL) and 1% (w/v) BSA for the positive and negative control, respectively (A). The certain current comparison after background subtraction (B). Nyquist plot comparison of the modified electrode using the adjusted EIS conditions: frequency range of 100 kHz to 0.01 Hz, 0.1 V potential and 0. 01 V perturbation amplitude in 5 mM $Fe(CN)_6^{4-/3-}$ (C). Cyclic voltammograms comparison of SPGE, GO-SPGE, AB1-GO-SPGE, AB1-SKI-GO-SPGE and LipL32-AB1-SKI-GO-SPGE (D). The reaction solution was 5 mM [$Fe(CN)_6$]$^{4-/3-}$ containing 0.1 M KCl solution, scan rate: 50 mV s^{-1}.

3.2. Electrochemical detection of LipL32 by using the developed immunosensor

The electrochemical detection of LipL32 was performed by DPV using a gold signal response as an indicator. As displayed in Fig. 2A, after exposure of the prepared immunosensor to the LipL32 solution and subsequent binding with the signaling antibody, a characteristic Au peak apparently appeared at +0.4 V, while only negligible response was observed in a negative control. This result demonstrated that the immunosensor successfully detected LipL32. However, after considering a negative control signal, there was a small peak appeared (~0.1 µA). This might be due to there is non-specific adsorption occurred on the electrode surface. Nevertheless, to obtain a certain signal, the current response will be background subtracted as shown in Fig. 2B. All the current plots against concentrations in the presence of LipL32 was background subtraction current.

Furthermore, EIS technique was employed to further verify the successful fabrication of sensor in a step-by-step fashion. The semicircle diameters reflect the electron-transfer resistance (R_{et}) at the electrode interface, controlling the electron-transfer kinetics of the redox probe employed ([$Fe(CN)_6$]$^{4-/3-}$) (Lisdat and Schafer, 2008). As presented in Fig. 2C, the unmodified SPGE provided a smaller semicircle with an R_{et} of 8.58 kΩ (%RSD) = 2.43) (SPGE) compared to the GO-SPGE that exhibited a nonlinear line with an extremely high R_{et} of 19.19 kΩ (% RSD = 3.22) (GO-SPGE) at high frequencies since GO casted on the electrode surface is a semiconductor by property (Stankovich et al., 2007). This clearly demonstrated that GO was successfully casted onto the electrode surface. When the anti-LipL32 surface was successfully constructed, a 23.75 kΩ (%RSD = 5.01) (AB1-GO-SPGE) increase in R_{et} was observed. In addition, the R_{et} was found to further increase to 30.02 kΩ (%RSD = 2.56) (AB1-SKI-GO-SPGE) after the blocking step. The R_{et} increment can be explained by the blocking of the electrode surface by the anti-LipL32 barrier and the adopted blocking agent, making it less accessible for the $Fe(CN)_6^{4-/3-}$ redox couple. Additionally, the R_{et} value was remarkably increased to 43.28 kΩ (% RSD = 6.11) (LipL32-AB1-SKI-GO-SPGE) after the addition of target protein. This is attributed to the shielding effect of the immunocomplexes (antibody-antigen) on the electrode surface and the negative charge of carbonaceous nanomaterials including graphene, which resulted in an additional increase in the negatively charged of the electrode surface (Feng et al., 2013; Jampasa et al., 2018b). Therefore, the shielding barrier to the negatively charged $Fe(CN)_6^{4-/3-}$ redox couple increased, causing an increase in the charge-transfer resistance.

From the relationship between R_{et} and the heterogeneous electron-transfer rate constant (K_{et}) according to equation (1), the K_{et} value of each electrode could be successfully obtained (Bradbury et al., 2010; Jampasa et al., 2016).

$$K_{et} = \frac{RT}{n^2F^2R_{et}AC_{redox}} \quad (1)$$

A is the geometrical area of the electrode surface, and C_{redox} corresponds to the concentration of the $Fe(CN)_6^{4-/3-}$. The K_{et} values were calculated to be 0.88×10^{-5} cm s^{-1}, 0.39×10^{-5} cm s^{-1}, 0.32×10^{-5} cm s^{-1}, 0.25×10^{-5} cm $s^{-1}$and 0.17×10^{-5} cm s^{-1} for the SPGE, GO-SPGE, AB1-GO-SPGE, AB1-SKI-GO-SPGE and LipL32-AB1-SKI-GO-SPGE, respectively.

In addition, the successful modification of electrode was verified by CV (Fig. 2D). The results were consistent with EIS, confirming the successful fabrication of LipL32 immunosensor (Emran et al. 2018b, 2018c, 2018d; Wang et al., 2014). More explanation of CV results can be found in SI, section 1.9.

3.3. Influence of variable parameters

Our proposed immunosensor is mainly focused on its application in human system in which the optimal pH in biological fluid is around 7.4. We conducted the experiment using this pH condition, hence, there is no further experiment is attempt. The optimization was completed with the adjusted DPV condition: 60 mV amplitude, 50 mV s^{-1} scan rate and 10 mV step potential. The amplitude interval was studied in the range from 10 to 80 mV, and the step potential was varied from 2 to 20 mV (Figs. S5 and SI).

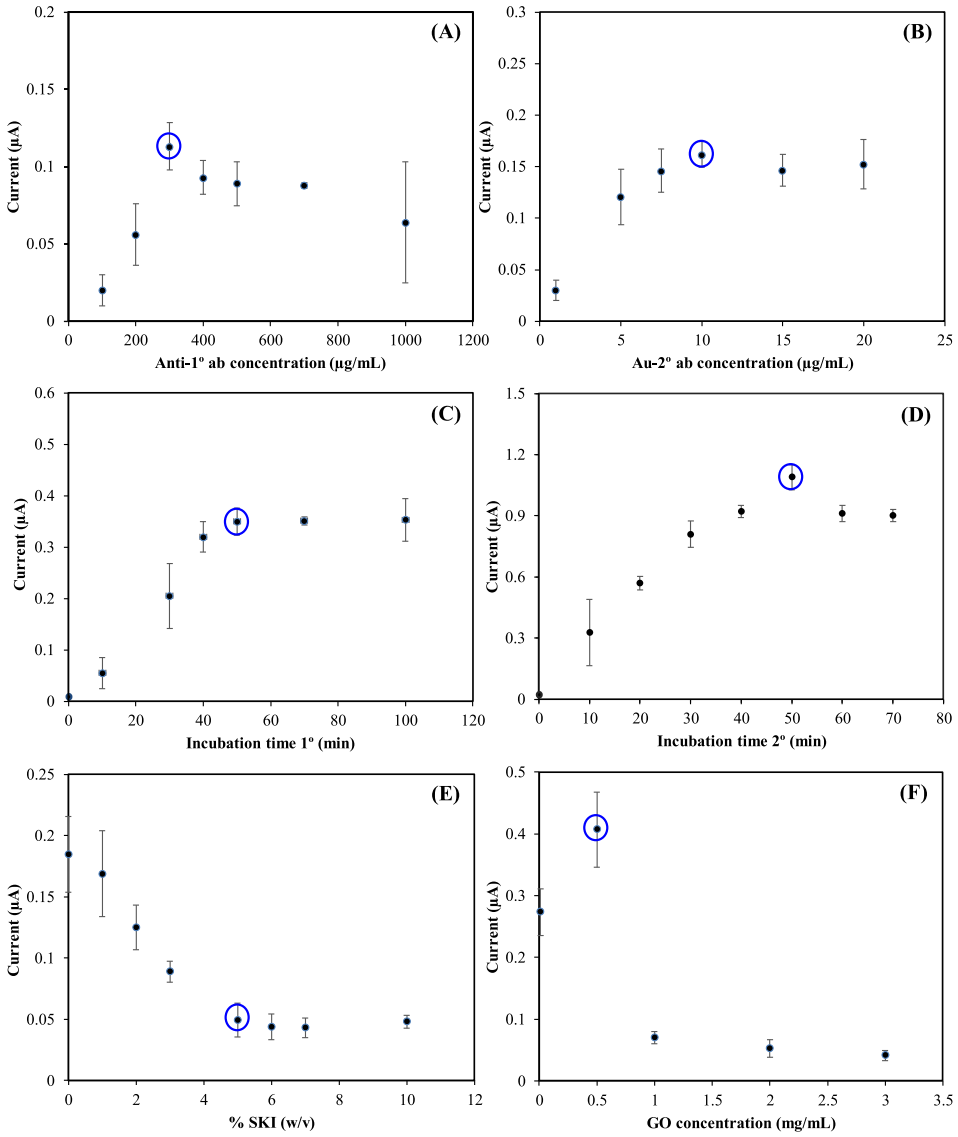

Fig. 3. Optimization of variable parameters: capture anti-LipL32 concentration (from 100 to 1000 μg/mL) (A), signaling antibodies (from 1 to 20 μg/mL) (B), the first incubation time (from 0 to 100 min) (C), the second incubation time (from 0 to 70 min) (D), SKI loading amount (from 0 to 10 %w/v) (E), GO concentration (from 0.01 to 3 mg/mL) (F), at 30 ng/mL of LipL32, using DPV in 0.5 M HCl.

3.3.1. The capture (Anti-1°Ab) and signaling anti-LipL32 (Au-2°Ab) concentrations

The concentrations ranging from 100 to 1000 μg/mL and 1–20 μg/mL were investigated for the capture and signaling antibody, respectively. The current response progressively increased with increasing both capture (Fig. 3A) and signaling anti-LipL32 antibody concentrations (Fig. 3B), and then reached the maximum value at 300 μg/mL and 10 μg/mL, respectively. The plateau signal was explained by an oversaturation of the electrode surface at conditions above these limits, and thus, there are a limited number of conjugated anti-LipL32/LipL32 complexes that could be formed on the electrode surface (Clark and Adams, 1977). Thus, 300 and 10 μg/mL were the optimal concentrations for the capture and signaling antibodies, respectively. These conditions were chosen for the further experiments.

3.3.2. The first and second incubation time

The incubation time was studied in the time range from 0 to 100 min. The results showed that the current signal gradually increased within 50 min for both the first (Fig. 3C) and second (Fig. 3D) incubation time. The current response signals for both incubation steps tended to reach a plateau after 50 min, which could also be described by the limited number of immunocomplexes formed on the electrode surface (Clark and Adams, 1977). Hence, 50 min was therefore selected as an appropriate time for both first and second incubation.

3.3.3. Effect of blocking agent type and concentration

The surface blocking is a crucial step of immunoassay, since it prevents antibodies and other interferences from nonspecific binding (Xiao and Isaacs, 2012). The results revealed that the background signal was significantly influenced by type of the blocking agents used, BSA and SKI (5% w/v). The sensor constructed with SKI offered a small background signal (close to zero or lower than 0.1 μA), indicating that the highest efficiency of surface blocking was achieved (Figs. S6 and SI) (Babcock and Brancaleon, 2013; Etzel, 2004). As displayed in Fig. 3E, it was also found that at 5% (w/v) of SKI was the optimal condition, hence, this concentration was selected for all further experiments. More description of this parameter can be seen in SI, section 1.11.

3.3.4. Influence of GO concentration

The amount of carboxylate groups on the transducer surface can directly introduce by varying of the concentration of GO in the dispersed media. To accomplish the proper conditions for the detection, an

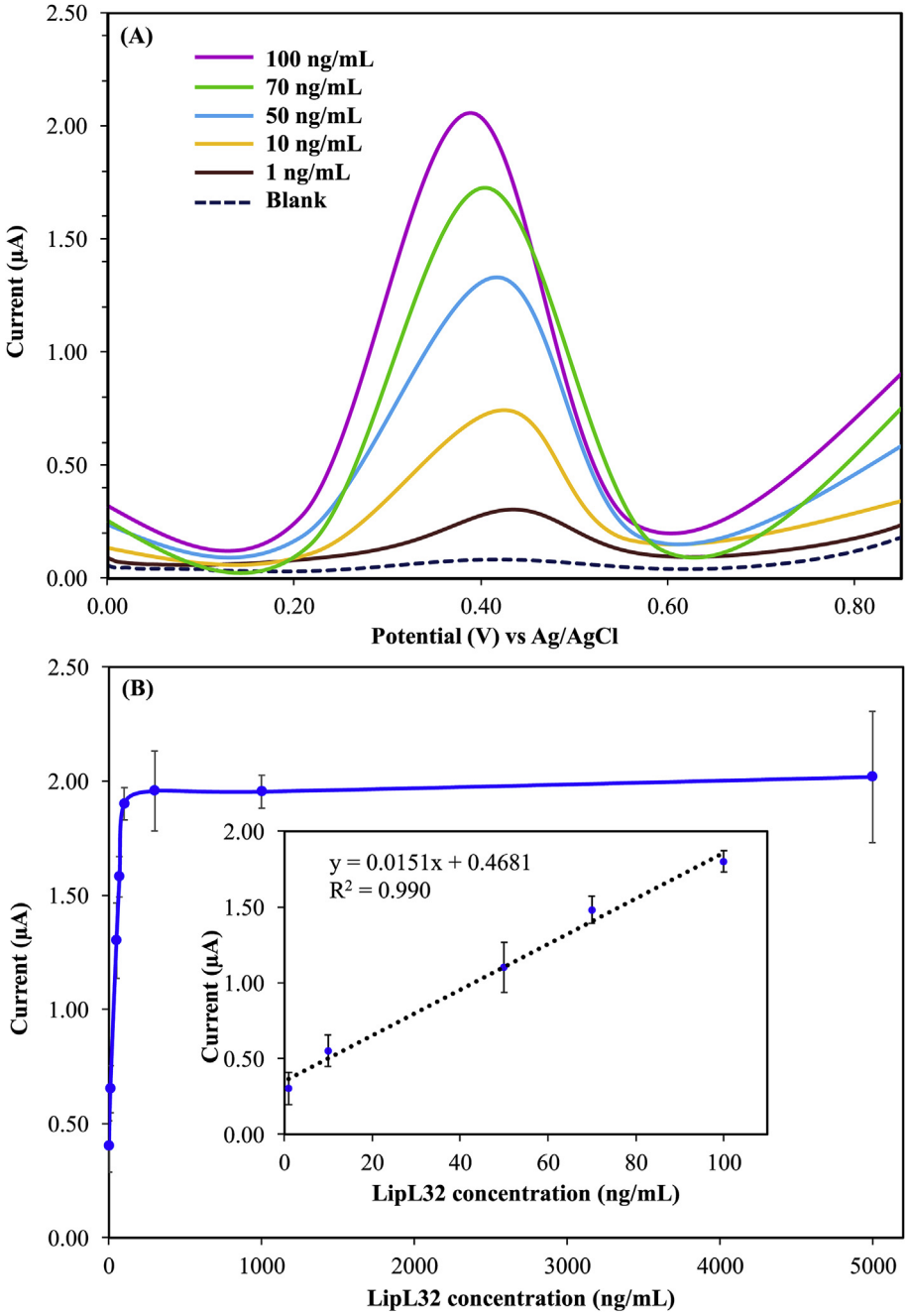

Fig. 4. Representative DPV of the AB1-SKI-GO-SPGE after addition of the target LipL32 (1–100 µg/mL) (A). Plot of current response vs. the concentrations of LipL32 from 1 to 5000 ng/mL (B) and from 1 to 100 ng/mL (inset).

effect of GO concentration was carefully evaluated. As the result obtained, a gradual increase in GO concentrations from 0.01 to 0.5 mg/mL resulted in remarkable increases in the current response of gold-conjugated signaling antibody (Fig. 3F). During this period, the number of carboxylate group significantly increased, resulting in an abundance of antibody anchoring sites on the electrode surface and a gradual increase in current responses. This signal then reached the maximum at 0.5 mg/mL of GO. Nevertheless, the currents response signal dramatically decreased as the GO concentration was increased from 1 to 3 mg/mL (Stankovich et al., 2007). This evidence indicated that 0.5 mg/mL of GO was an optimal condition.

3.4. The analytical performances of the immunosensor

After the formation of Anti-1˚Ab-GO-SPGE, a calibration plot of the current response signal at different LipL32 concentrations ranging from 1 ng/mL to 5000 ng/mL was constructed (Fig. 4B). As expected, a higher DPV current response signal was observed when the modified electrode was exposed to higher LipL32 concentration (Fig. 4A), and the calibration curve was linear over a range from 1 to 100 ng/mL with an R^2 value of 0.99 (Fig. 4 (inset)). The limit of detection (LOD) ($3SD_{blank}$/slope) was found to be 0.28 ng/mL. Likewise, from this data, the limit of quantitation (LOQ) ($10SD_{blank}$/slope) were calculated to be 0.93 ng/mL. Nonetheless, compared to other traditional methods and strategies, the advantages of this developed sensor were simple, inexpensive, disposable and it requires small sample volume, which makes it very

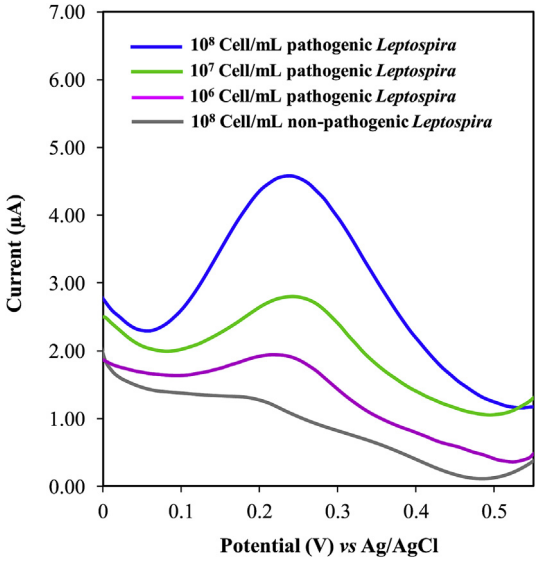

Fig. 5. Comparison of DPV signals response of the developed LipL32 immunosensor in the presence of various examined pathogenic *Leptospira* concentrations.

attractive for rapid point-of-care applications. Disadvantages of this immunosensor include the necessity of immobilizing the antibody and the rather high detection limit by the standard of pathogenic detection. Nevertheless, its performance is adequately good to allow examination of pathogenic Leptospira whole cell lysates samples.

In addition, the selectivity of the developed method was also evaluated. Human serum with various concentrations was employed as an interference in this study. It was found that the signal was observed only in the presence of LipL32 and was negligible for the three-spiked human serum (Figs. S7 and SI). The %RSD was found to be less than 5%, which were acceptable. These signal responses indicated that the proposed immunosensor has a high selectivity and specificity.

3.5. Stability and reproducibility of the proposed method

To demonstrate stability of the developed LipL32 immunosensor, the storage lifetime was then investigated. The prepared sensor was kept in a refrigerator at 4 °C until use. The result revealed that the signal response was stable within 2 weeks with the percentage of the decreased signal less than 10% (%RSD = 4.8). However, the signal was significantly decreased in comparison to the original signal after 14 days (Figs. S8 and SI). The result obtained indicated that the proposed method has good stability for up to 2 weeks.

In addition, to achieve reliable and accurate results, reproducibility (expressed as the %RSD of repetitive measurements (n = 7)) of the present method was examined. The tested sensors were prepared using the same procedure and subsequent electrochemical measurements of LipL32 concentrations at 10, 50 and 70 ng/mL (n = 7) were recorded. It was found that an exceptional reproducibility was obtained for the detection of LipL32, where %RSD was found to be less than 5%. This value indicated that the constructed immunosensor has remarkably low sensor-to-sensor deviation with an excellent fabrication reproducibility.

3.6. Application in real sample

To demonstrate the applicability of this developed immunosensor, the pathogenic (10^8 cell/mL) and non-pathogenic (10^8 cell/mL) *Leptospira* whole cell lysates samples was consequently tested for the positive and negative control, respectively. A serial dilution (10^7 and 10^6 cell/mL) of these samples was prepared in PBS buffer of pH 7.4. As expected, the current signal response obviously increased in a pathogenic *Leptospira* concentration-dependent manner, but negligible signal response was observed in all cases of the non-pathogenic *Leptospira* (Fig. 5). Based on the obtained results, it can be concluded that this novel sensing platform was successfully applied to detect the pathogenic and failed to detect the non-pathogenic *Leptospira*. In contrast, it can be stated that the detection limit of this developed immunosensor is sufficient to allow for detection of the pathogenic *Leptospira* in the patients diagnosed with Leptospirosis. Hence, our proposed approach can be used as a new and reliable alternative assay for the selective and rapid screening of LipL32 in early diagnosis of Leptospirosis.

4. Conclusions

An electrochemical immunosensor for LipL32 detection based on a gold-labeled monoclonal anti-LipL32 was successfully fabricated. The current response signal was obviously increased only in the presence of the target protein. The calibration curve of this developed immunosensor exhibited a linear correlation of 1–100 ng/mL, and the corresponding LOD and LOQ were found to be 0.28 and 0.93 ng/mL, respectively. This immunosensor platform showed the high stability for up to 2 weeks with the percentage of the decreased signal less than 10%. In addition, an exceptional reproducibility was obtained for the detection of LipL32, where %RSD was found to be lower than 5%, indicating that an excellent fabrication reproducibility. For practical analysis, this developed sensor was successfully applied to detect pathogenic *Leptospira* whole cell lysates samples with the satisfactory results. The main advantages of this platform include the ease of fabrication, rapid analysis with simple instrument. Furthermore, this electrode can also be prepared inexpensively, and it requires low sample volume (2.5 µL). Hence, this present technique might be suitable as a novel device for LipL32 screening in the early diagnosis of Leptospirosis.

Acknowledgments

Dr. Sakda Jampasa would like to acknowledge to Rachadapisek Sompote Fund Chulalongkorn University for postdoctoral fellowship and thank Science Achievement Scholarship of Thailand (SAST) for supports. The authors also thank the Thailand Research Fund via the Research Team Promotion Grant (RTA6080002) for the financial support.

Appendix A. Supplementary data

Supplementary data to this article can be found online at https://doi.org/10.1016/j.bios.2019.111539.

Declaration of interests

The authors declare that they have no known competing financial interests or personal relationships that could have appeared to influence the work reported in this paper.

References

Anne, A., Bouchardon, A., Moiroux, J., 2003. J. Am. Chem. Soc. 125 (5), 1112–1113.
Babcock, J.J., Brancaleon, L., 2013. Int. J. Biol. Macromol. 53, 42–53.
Basirun, W.J., Sookhakian, M., Baradaran, S., Mahmoudian, M.R., Ebadi, M., 2013. Nanoscale Res. Lett. 8 (1) 397-397.
Bayat, A.A., Ghods, R., Shabani, M., Mahmoudi, A.R., Yeganeh, O., Hassannia, H., Sadeghitabar, A., Balay-Goli, L., Noutash-Haghighat, F., Sarrafzadeh, A.R., Jeddi-Tehrani, M., 2015. Avicenna J. Med. Biotechnol. (AJMB) 7 (1), 2–7.
Bharti, A.R., Nally, J.E., Ricaldi, J.N., Matthias, M.A., Diaz, M.M., Lovett, M.A., Levett, P.N., Gilman, R.H., Willig, M.R., Gotuzzo, E., Vinetz, J.M., 2003. Lancet Infect. Dis. 3 (12), 757–771.
Bradbury, C.R., Kuster, L., Fermín, D.J., 2010. J. Electroanal. Chem. 646 (1), 114–123.
Budihal, S.V., Perwez, K., 2014. J. Clin. Diagn. Res. 8 (1), 199–202.

Clark, M.F., Adams, A.N., 1977. J. Gen. Virol. 34 (3), 475–483.
Daher, E.F., Silva, G.B., Silveira, C.O., Falcão, F.S., Alves, M.P., Mota, J.A.A.A., Lima, J.B., Mota, R.M.S., Vieira, A.P.F., Pires, R.d.J., Libório, A.B., 2014. Clinics 69 (2), 106–110.
De Souza, D., Machado, S.A.S., 2005. Anal. Chim. Acta 546 (1), 85–91.
Emran, M.Y., El-Safty, S.A., Shenashen, M.A., Minowa, T., 2019. Sens. Actuators B Chem. 284, 456–467.
Emran, Mohammed Y., Mekawy, M., Akhtar, N., Shenashen, Mohamed A., El-Sewify, Islam M., Faheem, A., El-Safty, Sherif A., 2018a. Biosens. Bioelectron. 100, 122–131.
Emran, M.Y., Shenashen, M.A., Abdelwahab, A.A., Abdelmottaleb, M., El-Safty, S.A., 2018b. New J. Chem. 42 (7), 5037–5044.
Emran, M.Y., Shenashen, M.A., Abdelwahab, A.A., Abdelmottaleb, M., Khairy, M., El-Safty, S.A., 2018c. Electrocatalysis 9 (4), 514–525.
Emran, M.Y., Shenashen, M.A., Abdelwahab, A.A., Khalifa, H., Mekawy, M., Akhtar, N., Abdelmottaleb, M., El-Safty, S.A., 2018d. J. Appl. Electrochem. 48 (5), 529–542.
Emran, M.Y., Shenashen, M.A., Morita, H., El-Safty, S.A., 2018e. Adv. Healthc. Mater. 7 (16), e1701459.
Emran, M.Y., Shenashen, M.A., Morita, H., El-Safty, S.A., 2018f. Biosens. Bioelectron. 109, 237–245.
Etzel, M.R., 2004. J. Nutr. 134 (4), 996s–1002s.
Feng, D., Lu, X., Dong, X., Ling, Y., Zhang, Y., 2013. Microchim. Acta 180 (9), 767–774.
Goarant, C., 2016. Res. Rep. Trop. Med. 7, 49–62.
Goyal, R.N., Gupta, V.K., Oyama, M., Bachheti, N., 2006. Electrochem. Commun. 8 (1), 65–70.
Haake, D.A., Chao, G., Zuerner, R.L., Barnett, J.K., Barnett, D., Mazel, M., Matsunaga, J., Levett, P.N., Bolin, C.A., 2000. Infect. Immun. 68 (4), 2276–2285.
Hammond, J.L., Formisano, N., Estrela, P., Carrara, S., Tkac, J., 2016. Essays Biochem. 60 (1), 69–80.
Hoke, D.E., Egan, S., Cullen, P.A., Adler, B., 2008. Infect. Immun. 76 (5), 2063–2069.
Huang, Y., Xu, J., Liu, J., Wang, X., Chen, B., 2017. Sensors 17 (10), 2375.
Izumi, Y., Fukazawa, T., Sugiyama, Y., Yagami, K., Urano, T., Tanikawa, T., 1991. Jikken dobutsu. Exp. Anim. 40 (3), 367–373.
Jabbar, A., Yasin, G., Khan, W.Q., Anwar, M.Y., Korai, R.M., Nizam, M.N., Muhyodin, G., 2017. RSC Adv. 7 (49), 31100–31109.
Jampasa, S., Siangproh, W., Duangmal, K., Chailapakul, O., 2016. Talanta 160, 113–124.
Jampasa, S., Siangproh, W., Laocharoensuk, R., Vilaivan, T., Chailapakul, O., 2018a. Talanta 183, 311–319.
Jampasa, S., Siangproh, W., Laocharoensuk, R., Yanatatsaneejit, P., Vilaivan, T., Chailapakul, O., 2018b. Sens. Actuators B Chem. 265, 514–521.
Jampasa, S., Wonsawat, W., Rodthongkum, N., Siangproh, W., Yanatatsaneejit, P., Vilaivan, T., Chailapakul, O., 2014. Biosens. Bioelectron. 54, 428–434.
Kuang, H., Chen, W., Xu, D., Xu, L., Zhu, Y., Liu, L., Chu, H., Peng, C., Xu, C., Zhu, S., 2010. Biosens. Bioelectron. 26 (2), 710–716.
Lisdat, F., Schafer, D., 2008. Anal. Bioanal. Chem. 391 (5), 1555–1567.
Mao, Y., Luo, C., Ouyang, Q., 2003. Nucleic Acids Res. 31 (18) e108-e108.
Musso, D., La Scola, B., 2013. J. Microbiol. Immunol. Infect. 46 (4), 245–252.
Raghav, R., Srivastava, S., 2016. Biosens. Bioelectron. 78, 396–403.
Stankovich, S., Dikin, D.A., Piner, R.D., Kohlhaas, K.A., Kleinhammes, A., Jia, Y., Wu, Y., Nguyen, S.T., Ruoff, R.S., 2007. Carbon 45 (7), 1558–1565.
Sumarningsih, Tarigan, S., Susanti, Kusmiyati, 2016. Procedia Chem. 18, 18–25.
Wang, J., 2006. Biosens. Bioelectron. 21 (10), 1887–1892.
Wang, L., Hua, E., Liang, M., Ma, C., Liu, Z., Sheng, S., Liu, M., Xie, G., Feng, W., 2014. Biosens. Bioelectron. 51, 201–207.
Wei, H., Sun, J.-J., Xie, Y., Lin, C.-G., Wang, Y.-M., Yin, W.-H., Chen, G.-N., 2007. Anal. Chim. Acta 588 (2), 297–303.
Wu, Y., Lai, R.Y., 2013. Chem. Commun. 49 (33), 3422–3424.
Wu, Y., Lai, R.Y., 2015. Anal. Chem. 87 (21), 11092–11097.
Xiao, Y., Isaacs, S.N., 2012. J. Immunol. Methods 384 (1–2), 148–151.
Zhang, D., Liu, Q., 2016. Biosens. Bioelectron. 75, 273–284.
Zhang, J., Yang, H., Shen, G., Cheng, P., Zhang, J., Guo, S., 2010. Chem. Commun. 46 (7), 1112–1114.